Indian Journal of Engineering & Materials Sciences
Vol. 33, June 2026, pp. 312-323
DOI: 10.56042/ijems.v33i03.24137

# Optimization of effective chloride migration in mortar containing nano titanium dioxide using bio-inspired metaheuristics

Yogesh Iyer Murthy[a*] & Aditya Shrivastav[b]

[a]Department of Civil Engineering, Oriental College of Technology, Bhopal 462022, Madhya Pradesh, India

[b]Department of Computer Science Engineering, Jaypee University of Engineering and Technology, Guna 473226, Madhya Pradesh, India

*Received:23 September 2025; accepted: 15 February 2026*

This research has investigated the impact of nano-$TiO_2$ (NT) as a partial replacement for cement (0–3%) on chloride migration in cement mortar and has established a predictive framework utilizing advanced metaheuristic algorithms. Experimental results have indicated that an increase in NT content has markedly delayed the onset of steady-state diffusion, with the duration required to reach steady state having increased by approximately 45% at 3% NT, primarily as a result of pore refinement and matrix densification. The chloride diffusion coefficient has consistently been decreased with a lower water–cement ratio and a higher NT content, indicating enhanced resistance to chloride ingress. To accurately model this nonlinear behavior, ten metaheuristic algorithms have been employed: Bat Algorithm, Cuckoo Search, Differential Evolution, Harris Hawks Optimization, Grey Wolf Optimizer, Firefly Algorithm, Jaya, Moth–Flame Optimization, Multi-Verse Optimizer, and Particle Swarm Optimization, with the objective of minimizing mean squared error. Differential Evolution, Multi-Verse Optimizer, and Particle Swarm Optimization have achieved the fastest convergence, reducing the mean squared error to below 0.5 within 20 iterations, whereas Cuckoo Search, Grey Wolf Optimizer, Harris Hawks Optimization, and Jaya have demonstrated consistent and reliable performance. Thus, the integrated experimental and computational approach has provided a dependable data-driven framework for forecasting chloride transport in NT-modified mortar and has offered valuable insights into the design of durable and sustainable concrete.

**Keywords:** Cement mortar, Chloride migration coefficient, Metaheuristic optimization algorithms, Nano titanium dioxide

## 1 Introduction

Reinforced concrete buildings are utilized extensively in practical engineering applications, with the longevity of these structures being the primary focus of academic research[1, 2]. One of the key causes of the reduction in durability is the corrosion of steel reinforcement that is caused by chloride salts[3]. It has been proven through research that when steel is situated in a very alkaline environment, a passivation coating forms on the surface of the steel, maintaining a stable condition[4, 5]. However, when the structure is subjected to chloride environments for extended periods of time, chloride ions present in the external environment seep into the concrete surface and then diffuse from the concrete surface to the steel surface[6]. This occurs because of the concentration gradient.

Pitting corrosion of the surface of the steel occurs once the passivation coating transitions from a stable state to an active state once the chloride ion concentration at the surface of the steel beyond a certain threshold value[5-7]. There are two types of chloride ions that cause steel to corrode[8]. The first source is chlorides that are mixed into concrete, and the second source is chlorides that are from external surroundings, such as de-icing salts or marine settings[9]. Controlling the elements that are used in the concrete mix allows for optimization of the former, but the latter is influenced by factors that cannot be controlled. There are three different kinds of chloride ions that can be found in concrete: chemically bonded, physically adsorbed, and free. Of these three forms, free chloride is the primary cause of steel corrosion[9]. Corrosion diminishes the effective cross-sectional area of the steel, weakens the bond between the steel and concrete, and causes the volume of corrosion products at the steel/concrete interface to expand by 2–4 times, which leads to the cracking and spalling of the protective layer. This ultimately results in structural failure[10].

Recently, researchers have carried out a significant amount of study on the mechanisms of corrosion and chloride ion transport, as well as the factors that

*Corresponding author (E-mail: yogeshiyermurthy@oriental.ac.in)

influence them[10-12]. The models that are currently in use for chloride ion transport are derived from Fick's laws. Experiments have been used to modify these models to account for aspects such as the kind and amount of additives, ambient conditions, water-to-cement ratio, and chloride binding capacity[12]. Nevertheless, due to the fact that the existing models are still unable to fully capture the diffusion characteristics of chloride ions, this is caused by the complexity of the factors that influence the diffusion of chloride ions and the complicated nature of the transport and corrosion processes[13]. In addition, the corrosion caused by chloride ions has resulted in considerable structural damage, which has resulted in a major increase in maintenance expenses. To guarantee structural durability, much effort has been dedicated to investigating and implementing methods to avoid steel corrosion. It is possible to further reduce the transport of chloride ions in structures that are essential in hostile environments by employing suitable supplementary methods[13-17].The necessity for more precise and adaptable predictive models becomes apparent in light of these obstacles. Traditional Fickian-based techniques[18], despite being widely utilized, frequently fall short of completely capturing the combined impacts of microstructural refinement, chloride binding[19], and fluctuations in the time-dependent diffusion coefficient[20], particularly in cases when extra cementitious materials or nanomaterials are included[21-24]. Experimental data alone is a necessary component; nevertheless, it may not generalize well to a variety of exposure situations and mix designs. To accomplish this, it is necessary to construct computational models that are capable of learning complex, nonlinear correlations between many input factors, such as the dosage of NT, the ratio of water to cement, and the amount of time of exposure. These variables are all related to the features of chloride migration. Approaches utilizing soft computing and machine learning have proven to be viable options for overcoming these restrictions, providing data-driven modeling methodologies that are able to supplement experimental findings[25]. Among these strategies, metaheuristic optimization[26, 27] techniques that are inspired by natural phenomena are particularly noteworthy due to their ability to effectively navigate high-dimensional solution spaces, escape being trapped in local optima, and produce globally optimized models for the prediction of chloride ion transport with greater accuracy.

Thus, the application of nature-inspired metaheuristic optimization algorithms has gained prominence in civil engineering research for predicting and optimizing essential concrete qualities such as strength[28], permeability[29], and diffusivity[30]. Due to their resilience to local optima and formidable global search capabilities, algorithms such as Particle Swarm Optimization (PSO)[31], Differential Evolution (DE)[32], Grey Wolf Optimizer (GWO)[33], and Multi-Verse Optimizer (MVO)[32] have been effectively employed for parameter identification and model development in intricate, nonlinear systems. In the context of highly nonlinear data, these algorithms have exhibited superior performance compared to conventional regression methods by iteratively minimizing error functions through the simulation of biological, physical, or natural processes[33-37]. In this study, eleven algorithms—BAT, CS, DE, FFA, HHO, Jaya, MFO, MVO, PSO, SCA, and GWO—are employed to simulate the chloride migration coefficient of mortar incorporating varying dosages of NT (0–3%). This study evaluates the convergence behavior, accuracy, and stability of various algorithms to identify the optimal approach for predicting chloride ion diffusion and enhancing the incorporation of nano-admixture in cementitious composites, aimed at producing durable and sustainable cementitious materials.

The growing demand for long-lasting and sustainable concrete necessitates methods that use fly ash and other industrial byproducts, use less cement, and increase the concrete's resistance to corrosion caused by chloride. Although there is much promise for improving chloride diffusion resistance with nano-materials like NT, their efficiency is highly dependent on dose, which is frequently established through time-consuming trial-and-error trials. There has been very little research comparing a variety of metaheuristic optimization algorithms for predicting and optimizing the chloride migration coefficient, though, as the majority of prior studies have either concentrated on conventional statistical modeling or on the experimental evaluation of concrete modified with nano-materials. The nonlinear relationship between the chloride migration coefficient and nano-admixture content can be effectively modeled by computational intelligence, especially through nature-inspired metaheuristic optimization algorithms. This allows for precise prediction and optimization with less experimental work. Therefore, the following are the research significance of this work:

- To compare eleven cutting-edge metaheuristic algorithms (BAT, CS, DE, FFA, HHO, Jaya, MFO, MVO, PSO, SCA, and GWO) to estimate the chloride migration coefficient of mortar modified with nano-$TiO_2$, thereby filling the research gap to a considerable extent.
- To optimizeNT dosage for increased durability by using predictive modeling, this lessens the need for strictly experimental experiments.
- To provide thorough information about the correctness, stability, and convergence behavior of each algorithm, directing future material modeling applications and provide a generalized computational framework for intelligent mix design optimization that may be expanded to other material attributes (such as strength and permeability). Further, based on the above-mentioned research significance, the following are the major objectives of this research:
- To experimentally obtain the chloride migration coefficient of cement mortar containing 0–3% NT.
- To develop predictive models utilizing eleven nature-inspired optimization techniques and compare their MSE and convergence rates.
- To obtain the most reliable and efficient optimizer for this application by analyzing algorithm convergence behavior and determination of optimal NT dose for strong chloride migration resistance and suggest practical implementation.

## 2 Materials and Methods

Figure 1 illustrates the schematic arrangement of the chloride migration test cell employed to assess chloride ion diffusivity in cement mortar specimens, in accordance with Nord Test NT Build 492[38], ASTM C-1202[39], and AASHTO T277[40]. To establish an impermeable barrier between the compartments, cylindrical specimens with a diameter of 25 mm and a length of 100 mm were cured in water at 22 °C for 28 days and subsequently positioned within a 25 mm PVC pipe. According to Whiting[41] and Andrade[42], the catholyte chamber was filled with a 1 M NaCl solution as the source of chloride ions, whereas the anolyte chamber contained a 0.3 M NaOH solution to replicate the pore solution and inhibit specimen dissolving. Andrade *et al.*[42] observed that solute concentration is essential for obtaining valid results, since highly concentrated solutions restrict ion activity, whereas excessively dilute solutions diminish the driving force and may lead to inaccuracies. Each compartment contained 200 ml of solution. This investigation employed an activity value of 0.657 for 0.3 M NaCl. The cathode (negative terminal) was located in the NaCl chamber, while the anode (positive terminal) was situated in the NaOH chamber, sustaining a cell potential of 9 V. The specimen thickness for ion transport was 50 mm, with a symmetrical design maintaining a distance of 100 mm between the specimen and each electrode. Chloride ions transfer from the catholyte to the anolyte under these conditions, and thermodynamic and electrochemical factors such as ion concentration, activity coefficient, sample thickness, and Faraday's constant can be utilized to compute chloride flux (JCl).

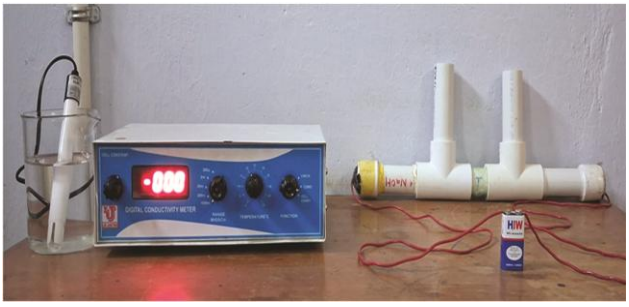


Fig. 1 — Set-up of the chloride migration test.

### 2.1 Algorithms used in this research

Based on the echolocation habits of microbats, the BAT is a bio-inspired metaheuristic[43]. The position, velocity, frequency, loudness, and pulse emission rate of each bat are considered to be characteristics of an agent. To balance exploration and exploitation, the program dynamically adjusts the positions of the bat and velocities while adjusting the loudness and pulse emission rate. Early on, high-frequency pulses enable worldwide exploration; later on, lower frequencies and less noise enable fine-tuning around favorable areas. When it comes to handling continuous optimization problems, BAT is renowned for its quick convergence, accurate solutions, and versatility. The brood parasitic behavior of cuckoo birds, which deposit their eggs in host bird nests, served as the inspiration for CS[44]. It performs random walks using Lévy flights, allowing for big exploratory leaps that avoid premature convergence. Whether a nest is abandoned and a fresh solution is used in its stead is determined by a discovery probability parameter. This technique works well for multimodal optimization when there are several local optima since it is straightforward, reliable, and has a strong global search capability.

A population-based evolutionary technique called DE[45,46] uses mutation, crossover, and selection operators to repeatedly improve potential solutions in order to optimize a problem. The weighted difference of two population vectors is added to a third vector to create a new candidate solution (mutant vector). Crossover comes next in order to boost variety and selection in order to keep better solutions. DE is one of the most dependable algorithms for continuous optimization problems because of its well-known simplicity, effectiveness, and robust convergence characteristics. The FFA[47] mimics the flashing behavior of fireflies, in which brightness is correlated with solution quality and attractiveness is proportionate to brightness. The beauty of a firefly decreases exponentially with distance as it approaches brighter (better) fireflies. To improve exploration, a randomization factor is also used. Because many fireflies can converge toward distinct local optima, this method naturally performs multimodal optimization, which makes it helpful for concurrently identifying numerous viable solutions. The cooperative hunting approach of HHO[48], which dynamically alternate between exploration and exploitation depending on the prey's fleeing energy, served as the model for Harris Hawks Optimization. It simulates many stages of hunting, including surprise pounce, strong besiege, and soft besiege. The algorithm progressively moves from global search (exploration) to local exploitation by varying the energy level parameter, which results in effective convergence. For highly nonlinear optimization situations, HHO works especially well. Based on the idea of iteratively advancing toward the best answer and away from the worst, the Jaya algorithm[49] is a parameterless optimization technique. Without requiring control parameters like crossover rates or mutation factors, each candidate solution is modified to increase its fitness. It is appealing for many scientific and technical optimization issues due to its consistency, simplicity, and lack of algorithm-specific parameters. The transverse orientation—the way moths fly in a spiral pattern around light sources—is the model for MFO[50]. To balance exploration and exploitation, candidate solutions (moths) update their positions in logarithmic spiral trajectories around a collection of flames (best solutions). The number of flames diminishes with each repetition, enabling convergence to areas that show promise. MFO works well for multimodal and large-scale issues.

The cosmological ideas of white holes, black holes, and wormholes—which stand for exploration, exploitation, and local search, respectively—are the foundation of the multi-verse optimizer (MVO)[51]. Wormhole operators randomly disturb solutions to promote exploration, whereas white hole mechanisms allow higher inflation-rate universes (better solutions) to communicate information with lower inflation-rate universes (bad solutions). MVO works effectively in complicated and high-dimensional optimization environments and has a significant capacity for diversification. PSO[52] draws inspiration from the social behavior of fish schools and flocks of birds. Every particle is a possible solution, and it modifies its position according to both its individual best-known position and the swarm's global best position. To balance exploration and exploitation, the velocity update equation takes into account inertia, cognitive (personal best), and social (global best) factors. Because of its simplicity, quick convergence, and convenience of usage, PSO is frequently used.

Using sine and cosine functions, the SCA[53] is a population-based mathematical optimizer that modifies candidate solutions to get them closer or further away from goal points. Step size is controlled by oscillation frequency and amplitude, which promotes global exploration in early iterations and exploitation afterward. SCA works well for a range of optimization tasks because of its straightforward process and seamless transition between exploration and exploitation. The hunting style and leadership structure of grey wolves served as the model for the Grey Wolf Optimizer (GWO)[54,55]. It simulates social dominance and hunting behavior, such as encircling prey, hunting, and attacking, by modeling four different wolf kinds (α, β, δ, and ω). By lowering a control parameter that regulates the encircling mechanism, the algorithm strikes a balance between exploration and exploitation while guaranteeing convergence to the prey (optimal solution). GWO is valued for its solid performance across benchmark functions, simplicity, and quick convergence. A concise description of these algorithms, along with the major mathematical equations and the important features are presented in Table 1.

To model the migration coefficient of NT modified mortar, these metaheuristic algorithms were chosen due to their complementary strengths in exploration, exploitation, and convergence behavior, which are essential for capturing the nonlinear relationship

Table 1 — Characteristics and mathematical formulations of the metaheuristic optimization algorithms employed for chloride migration prediction.

| S. No. | Algorithm | Inspiration | Key equations | Main features |
|---|---|---|---|---|
| 1 | BAT (Bat Algorithm) | Echolocation behavior of bats | $f_i = f_{min} + (f_{max} - f_{min})\beta$<br>$v_i^t = v_i^{t-1} + (x_i^{t-1} - x^*)f_i$<br>$x_i^t = x_i^{t-1} + v_i^t$ | Balances exploration through frequency tuning and exploitation through loudness and pulse-rate adaptation; suitable for continuous optimization. |
| 2 | CS (Cuckoo Search) | Brood parasitism and Lévy-flight behavior of cuckoos | $x_i^{t+1} = x_i^t + \alpha \oplus$ Lévy($\lambda$) | Uses Lévy flights for global exploration; simple structure with strong global-search capability. |
| 3 | DE (Differential Evolution) | Evolutionary mutation and crossover | $v_i = x_{r1} + F(x_{r2} - x_{r3})$<br>$u_{i,j} = v_{i,j}$, if $rand_j \leq C_r$; otherwise $x_{i,j}$ | Robust and computationally simple; highly effective for continuous and multimodal optimization problems. |
| 4 | FFA (Firefly Algorithm) | Attraction and flashing behavior of fireflies | $\beta = \beta_0 \exp(-\gamma r_{ij}^2)$<br>$x_i = x_i + \beta(x_j - x_i) + \alpha\varepsilon$ | Exploits brighter solutions while maintaining diversity through randomization; capable of avoiding local optima. |
| 5 | HHO (Harris Hawks Optimization) | Cooperative surprise-pounce hunting strategy of Harris hawks | $E = 2E_0(1 - t/T)$<br>$X(t+1) = X_{prey}(t) - E\lvert JX_{prey}(t) - X(t)\rvert$ | Uses adaptive exploration and exploitation phases based on prey energy; effective for complex nonlinear search spaces. |
| 6 | Jaya | Movement toward the best solution and away from the worst solution | $x_{i,j}^{new} = x_{i,j} + r_1(x_{best,j} - \lvert x_{i,j}\rvert) - r_2(x_{worst,j} - \lvert x_{i,j}\rvert)$ | Parameter-light algorithm; promotes convergence toward optimal solutions while avoiding poor solutions. |
| 7 | MFO (Moth-Flame Optimization) | Moth navigation around light sources | $D_i = \lvert F_j - M_i\rvert$<br>$M_i = D_i e^{bt}\cos(2\pi t) + F_j$ | Uses spiral movement to balance exploration and exploitation; effective for nonlinear optimization. |
| 8 | MVO (Multi-Verse Optimizer) | White holes, black holes, and wormholes in cosmology | $X_j^{i+1} = X_j^{rand}$, if $r < NI(U_i)$; otherwise $X_j^i$ | Employs probabilistic selection and wormhole mechanisms to maintain population diversity and improve global search. |
| 9 | PSO (Particle Swarm Optimization) | Collective behavior of birds and fish | $v_i^{t+1} = wv_i^t + c_1r_1(pbest_i - x_i) + c_2r_2(gbest - x_i)$<br>$x_i^{t+1} = x_i^t + v_i^{t+1}$ | Widely established and easy to implement; generally provides rapid convergence for continuous optimization. |
| 10 | SCA (Sine Cosine Algorithm) | Mathematical oscillatory behavior of sine and cosine functions | $X_i^{t+1} = X_i^t + r_1\sin(r_2)\lvert r_3P_i - X_i^t\rvert$<br>$X_i^{t+1} = X_i^t + r_1\cos(r_2)\lvert r_3P_i - X_i^t\rvert$ | Uses adaptive sine/cosine movements to alternate between exploration and exploitation. |
| 11 | GWO (Grey Wolf Optimizer) | Leadership hierarchy and cooperative hunting strategy of grey wolves | $D = \lvert C\cdot X_p - X\rvert$<br>$X(t+1) = X_p - A\cdot D$<br>$A = 2ar_1 - a$; $C = 2r_2$ | Mimics alpha, beta, and delta leadership; provides a simple balance between global exploration and local exploitation. |

between NT replacement levels and chloride transport properties differential evolution, particle swarm optimization, and multi-verse optimizer were chosen because they rapidly converge to near-global optima with minimal mean squared error, ensuring good prediction accuracy even for tiny experimental datasets. Cuckoo Search, Grey Wolf Optimizer, Harris Hawks Optimization, and Jaya were included for their robust exploration mechanisms and population diversity, which prevent premature convergence in complex, multimodal solution spaces typical of microstructural transport modeling. Although slower, the Bat Algorithm and Firefly Algorithm were designed to search deeper and verify solution stability, providing more global landscape exploration insights. Moth–Flame Optimization was chosen for its logarithmic spiral search trajectory that balances local refinement and global exploration, speeding convergence. This diversified group of algorithms benchmarks optimization performance, guaranteeing that the final model is correct and generalizable across NT replacement percentages (0–3%) and water–cement ratios. Comparing these methods helps determine the most computationally efficient and reliable durability modeling method for cementitious materials research.

## 3 Results and Discussion

This section involves a detailed discussion on the experimentally obtained values followed by the results obtained from various optimization algorithms.

### 3.1 Cumulative $Cl^-$ ion concentration in anolyte

Figure 2 (a-g) shows the cumulative chloride concentrations in anode cells for various mixes. The cumulative chloride concentration in anode cell of three duplicate samples exhibited remarkable

repeatability for a given percentage of NT. When chloride approaches steady-state diffusion, the ca/t (slope) is computed by linear regression using the Nordtest Build[38] technique. In this study, the steady state diffusion starting point was determined when the measured cumulative chloride concentration was more than 0.1 g/L[39]. The cumulative chloride concentration profiles in Fig. 2(a–g) explicitly demonstrate the significance of NT replacement levels (0, 0.5, 1, 1.5, 2, 2.5, and 3%) on chloride transport in cementitious composites. The high repeatability and reliability of the test method are confirmed by the virtually identical curves of the three duplicate samples for all mixtures. The control mix (0 % NT) represents the earliest onset of steady-state diffusion among all samples, as illustrated in Fig. 2(a).

The linear steady-state segment of this mix exhibits the highest slope (ca/t), which is indicative of the highest chloride diffusion coefficient. In comparison to the control, Fig. 2(b) illustrates a minor delay in the onset of steady-state diffusion and a marginal decrease in the ca/t slope. This corresponds to a 0.5 % NT replacement. The filler effect of NT is responsible for this enhancement, as it allows nano-particles to occupy capillary cavities and refine the pore structure. The presence of NT also accelerates cement hydration, resulting in the production of more C-S-H gel. This process reduces pore connectivity and delays chloride ingress. A more pronounced enhancement is evident in Fig. 2(c) for 1 % NT, as evidenced by a visibly delayed breakthrough point and a reduced slope, which suggests a lower effective diffusion coefficient. The dispersion of NT remains highly effective at this replacement level, resulting in a more homogeneous and dense microstructure. This densification is additionally facilitated by secondary hydration products, which obstruct transport channels and occupy voids.

The optimal overall performance is demonstrated in Fig. 2 (d) for 1.5 % NT, where the steady-state diffusion onset is considerably delayed and the ca/t slope is at one of its lowest points. This implies that the optimal equilibrium between hydration acceleration, pore refinement, and uniform particle dispersion is achieved at 1.5 % NT. It is probable that the microstructure at this dosage is the most compact, with minimal interconnected pores available for chloride ion transport, which explains the maximal reduction in diffusion coefficient. The cumulative concentration and ca/t slope of Fig.**2**(e) with 2 % NT are slightly higher than those of 1.5 % NT, though the chloride resistance remains outstanding. This suggests that the improvement is not as substantial beyond 1.5 percent, despite the fact that it is ongoing. At a higher NT content, dispersion becomes marginally more difficult, and agglomeration of nano-particles occurs. These agglomerates can function as micro-defects or faults that locally increase porosity and counteract the benefits of NT addition.

Figure 2 (f) at 2.5 % NT provides additional evidence of this trend, as the cumulative chloride concentration continues to increase slightly earlier than in the 1.5 % and 2 % NT cases. This indicates that the microstructural refinement benefit is approaching a plateau. The ca/t slope continues to be lower than the control, but it is no longer decreasing in proportion to the NT content. Further, Fig. 2(g) for 3 % NT demonstrates that chloride resistance is marginally less effective than 1.5 % NT, despite the fact that it is still superior to the control and 0.5 % combination. The modest increase in slope and the earlier onset of steady-state diffusion suggest that particle agglomeration and poor packing may result from excessive NT, thereby reducing the overall densification effect.

### 3.2 Diffusion test

Figure 3 presents the averaged values of $D_{eff}$ as a function of time t in both anolyte and catholyte for two identical migration tests. The diffusivity coefficient values are higher in the control mix, typically around $10^{\wedge-13}$ cm²/s, for both anolyte and catholyte[23]. With an increase in the percentage of NT, the pores within the mortar decrease due to the filler effect and enhanced microstructure, consequently diminishing the migration of Cl- ions[39]. The reduction in diffusivity values between the control mix and the mortar with 1% NT, 2% NT, and 3% NT at 15 minutes is 37.08%, 76.74%, and 90.4%, respectively. At the conclusion of the experiment, specifically at 105 minutes, the recorded values are 41.86%, 82.55%, and 90.3%[23]. Furthermore, as time progresses, the effective diffusion coefficient diminishes across all samples. Samples with 2% NT demonstrate clear observations. The chloride diffusivity coefficient in the anolyte cell varies over time for all NT replacement levels, as illustrated in Fig. 3(a). The control mix demonstrates the most rapid chloride migration, as evidenced by the highest diffusivity values throughout the entire test period. Since the control has a relatively coarser pore network

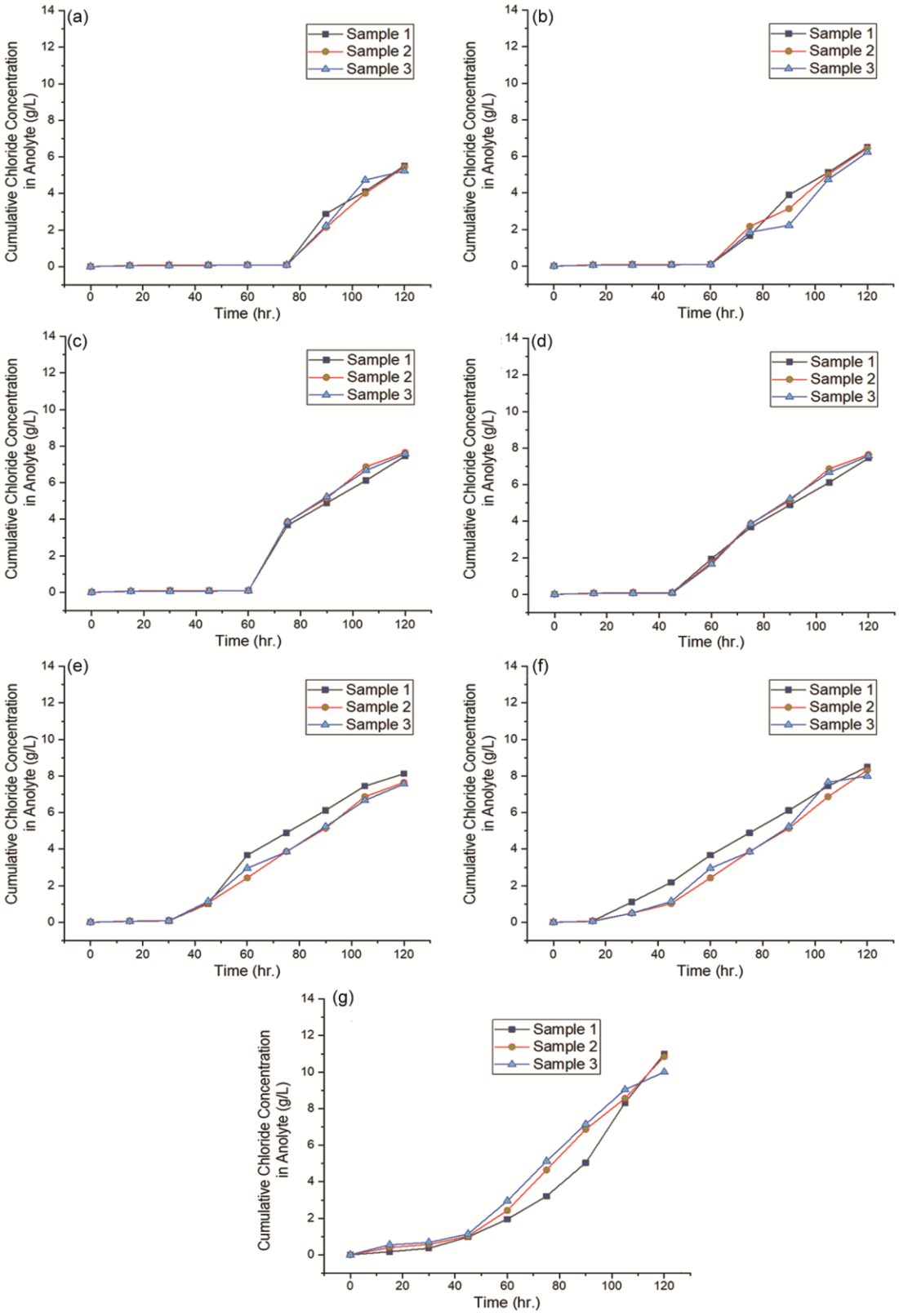



Fig. 2 — Cumulative chloride concentrations in anode cells (a) Control mix (0% NT), (b) 0.5 % NT, (c) 1% NT, (d) 1.5% NT, (e) 2% NT, (f) 2.5% NT, and (g) 3% NT replacement levels.

and higher capillary porosity, its curve rises sharply and stays above all NT-modified mixes, confirming its higher chloride transport capacity.

A systematic decrease in diffusivity is observed as the NT content increases from 0.5 % to 1.5 %, with the 1.5 % NT mixture exhibiting the most significant reduction. This suggests that the pore structure is effectively refined by the addition of NTup to this level, resulting in a denser microstructure with a more tortuous path for ion transport. The chloride movement is restricted and the steady-state diffusion is delayed by the finer pore structure. This enhancement is also influenced by the hydration acceleration induced by NT, which further diminishes the connectivity of larger capillary apertures by forming additional C–S–H gel layers. At 2 %, 2.5 %, and 3 %, the diffusivity continues to decrease, albeit at a reduced rate, beyond 1.5 %. This suggests that the improvement in chloride resistance has reached a plateau. This is most likely the result of particle agglomeration at higher concentrations, which diminishes their effective surface area and filler action. Nevertheless, the diffusivity is still substantially lower than the control at 3 % NT, indicating that NT continues to make a positive contribution to chloride resistance. The marginal benefit is believed to decrease after the optimal dosage (approximately 1.5%), as evidenced by the closely spaced curves for increased NT content (2–3%). Figure 3(b) illustrates the modulation of the diffusivity coefficient in the catholyte cell over time. The overall trend is a consistent decrease in diffusivity for all mixes as time progresses, which is indicative of the progressive depletion of chloride ions from the catholyte solution as migration continues. The control mix exhibits the maximum diffusivity values once more, while the NT-modified mixes consistently exhibit lower diffusivity. The relative spacing of curves is consistent with that in Fig. 3(a): the diffusivity decreases as the NT content increases, with the 1.5 % NT mix exhibiting the lowest diffusivity at nearly all time intervals. This further confirms that NT effectively reduces ionic permeability and improves the durability of the mortar system. It is important to note that the contours for 2 %, 2.5 %, and 3 % NT converge closely, suggesting that the effect of NT on diffusivity is approaching saturation. An intriguing result in Fig. 3(b) is the significant decrease in diffusivity that occurs between 400 and 800 minutes, following which the contours begin to stabilize. This is indicative of the transition to steady-state chloride diffusion, in which the concentration gradient between the two cells becomes nearly constant. This transition occurs slightly later for higher NT mixtures, as NT reduces pore connectivity, which is consistent with the delayed breakthrough observed in Fig. 2. The beneficial function of NT in reducing chloride diffusivity on both the anode and cathode sides of the migration cell is clearly established by Fig. 3(a & b) when considered in conjunction. The most substantial performance improvement is observed at 1.5 % NT, after which the reduction in diffusivity becomes less pronounced as a result of potential nanoparticle agglomeration. These findings verify that the replacement of NT results in a more refined and dense microstructure, which in turn

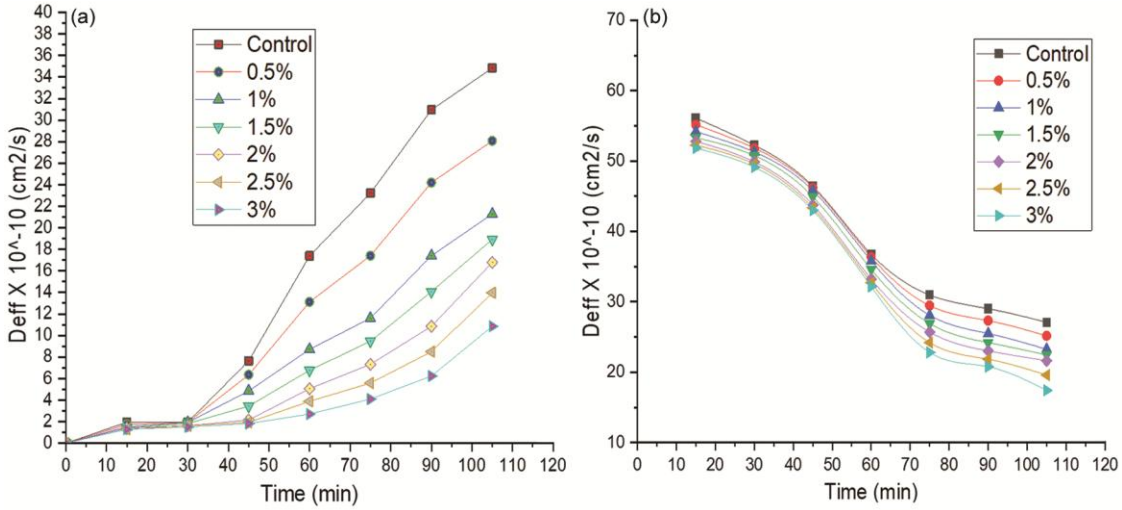



Fig. 3 — Plot of Diffusivity coefficient versus Time for duplicate experiments for (a) Anolyte, and (b) Catholyte.

reduces the rate of chloride ion transport and improves the long-term durability of the material against chloride-induced corrosion and 3% NT the diffusivity coefficients are significantly less, typically of the order of $10^{-14}$ ($cm^2/s$). Further, $D_{eff}$ values for anolyte and catholyte are less upto nearly 30 min for all the samples, after which the variations are more predominant.

The convergence behavior of the optimization algorithms illustrated in Fig. 4 (a–j) underscores their comparative effectiveness in minimizing the mean square error (MSE) throughout model training. Figure 4(a), which pertains to the BAT, illustrates a progressive decrease in mean squared error (MSE), beginning at approximately 4–4.5 and requiring nearly 20 iterations to drop below 2.0. Subsequently, the rate of improvement diminishes, stabilizing around 1.0–1.2 by the 100th iteration, reflecting a gradual transition from exploration to exploitation. Figure 4(b) illustrates the performance of CS, showing a rapid decline in MSE that falls below 1.0 within the initial 10 iterations and subsequently decreases to approximately 0.4–0.5 by the 60th iteration, indicating the effectiveness of Lévy flights in optimizing the balance between exploration and exploitation. Figure 4(c) illustrates that DE exhibits one of the highest convergence rates, with the MSE falling below 0.5 within 15 iterations and nearing zero by 30 iterations, demonstrating minimal variation across runs and indicating robust search efficacy. Figure 4(d) illustrates that the HHO exhibits a significant reduction in MSE during the initial 20 iterations, stabilizing between 0.4 and 0.6 with nearly overlapping trajectories, thereby indicating robust and

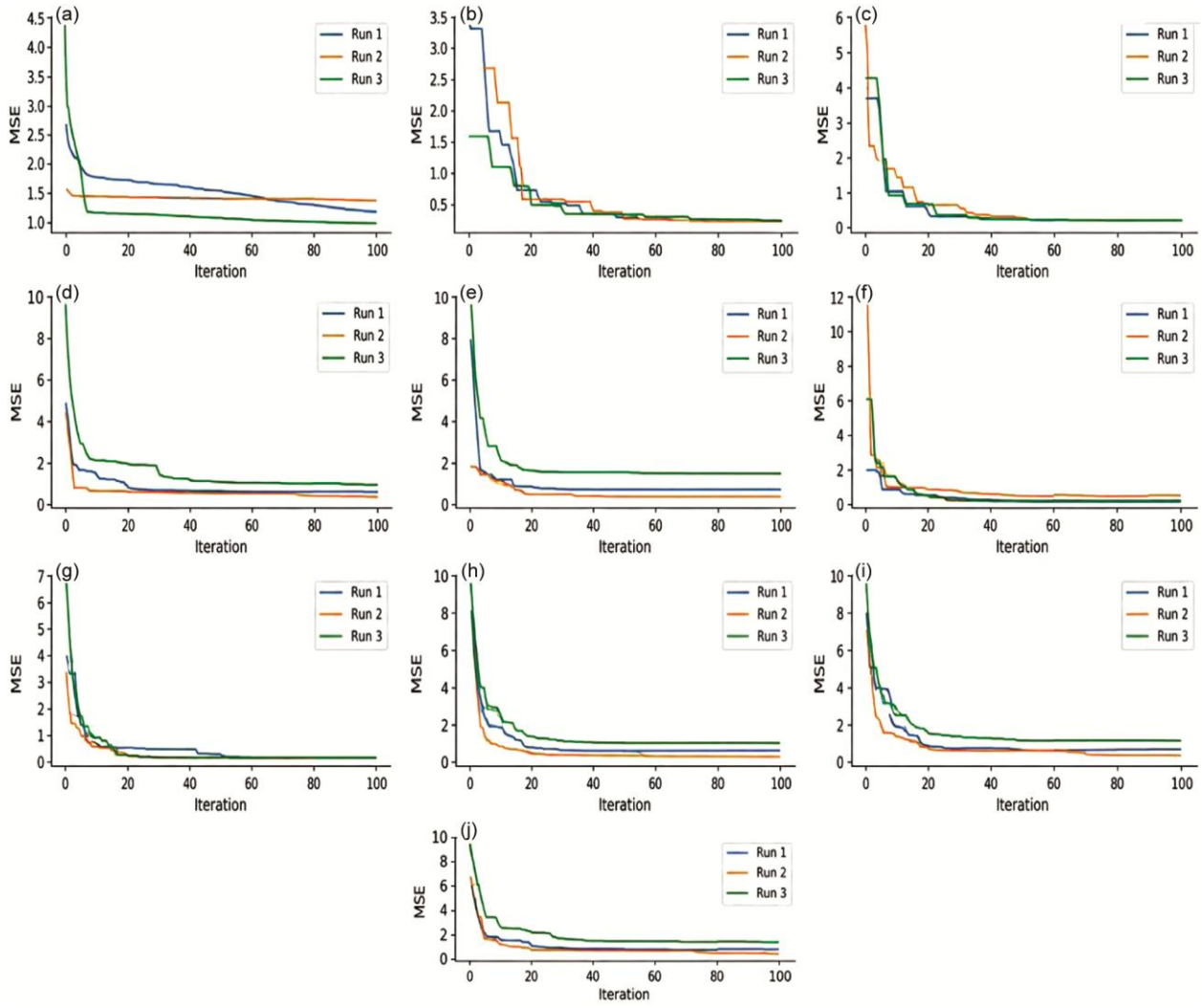



Fig. 4 — Convergence plots for (a) BAT, (b) CS, (c) DE, (d) HHO, (e) GWO,(f) FFA, (g) Jaya, (h) MFO, (i) MVO, and (j) PSO algorithms.

consistent convergence. Figure 4(e) illustrating the GWO shows a consistent decline below 1.0 over 25 iterations, accompanied by minimal variability between runs. This indicates that its encircling and hunting mechanisms facilitate a stable convergence without significant fluctuations. Figure 4(f) for the FFA indicates a high initial MSE, occasionally approaching 12, accompanied by a gradual convergence trend. It requires approximately 40 iterations to approach a value near 1.0, exhibiting significant variability across runs, which suggests sensitivity to initial parameter configurations and a slower exploitation of the search space. Figure 4(g) illustrates the Jaya algorithm, which exhibits a smooth and consistent convergence pattern, achieving values below 0.5 after approximately 35 iterations and final MSE in the range of 0.2 to 0.4 with minimal variability. This indicates its reliability, although it is somewhat slower than faster optimizerssuch as DE or MVO. Figure 4(h) illustrates the MFO process, demonstrating a significant reduction from approximately 6 to nearly 1.0 within 15 iterations. The approach rapidly converges to near-optimal solutions by around 30 iterations, suggesting the effectiveness of the logarithmic spiral-based exploitation strategy for this problem. Figure 4(i), which pertains to the MVO, demonstrates a significant decline, reaching nearly zero MSE after approximately 20 iterations with minimal variability. This outcome illustrates the ability of MVO to effectively balance exploration through white and black hole operators while ensuring robust intensification through wormhole mechanisms. Figure 4(j) illustrates that PSO achieves a rapid reduction from approximately 8 to below 0.5 within 10 iterations, subsequently converging smoothly to low MSE values with consistent performance across multiple runs. This outcome shows the effectiveness of its social learning behavior and the optimization of its convergence parameters. The results demonstrate that algorithms such as DE, MVO, PSO, and MFO exhibit high efficiency due to their robust operators, which facilitate swift global exploration and effective local exploitation, allowing for rapid convergence to the global optimum. The relatively slower convergence of CS, GWO, HHO, and Jaya indicates a greater investment of time in preserving population diversity. This strategy is beneficial for circumventing local minima, albeit requiring increased computational resources. BAT and FFA demonstrate the slowest convergence, attributed to their greater dependence on random exploration and reduced intensity of exploitation. This characteristic may necessitate additional iterations or parameter adjustments to attain similar accuracy levels. This study emphasizes the importance of accurately modeling the chloride migration coefficient at different NT replacement levels (0–3%). The rapid and consistent convergence of DE, MVO, and PSO effectively captures the impact of densification resulting from NT addition while maintaining minimal computational costs. The algorithms enable the model to accurately represent the observed experimental trends, indicating that increased NT percentages result in delayed steady-state chloride diffusion and reduced diffusion coefficients. The capacity to attain near-zero MSE rapidly guarantees that minor micro-structural alterations resulting from NT addition are accurately reflected in the prediction model, thereby enhancing the robustness and reliability of durability assessments for NT-modified mortar.

## 4 Conclusion

a The present investigation evaluated the impact of NT on the chloride migration resistance of cement mortar containing varying percentages of NT and developed predictive models for the chloride migration coefficient utilizing eleven metaheuristic optimization algorithms. The combination of experimental investigation and advanced computational modeling facilitated a thorough understanding of the relationship between NT dosage and Chloride migration, while also evaluating the efficiency of different algorithms. The following are the major conclusions of this research: Experimental results indicated that the incorporation of NT significantly enhanced the chloride migration resistance, the minimum value recorded being 5.8 $\times 10^{-12}$ m²/s at a concentration of 2% nano-$TiO_2$, indicating an approximate 38% reduction relative to the control mix.

b The evaluation of the eleven optimization algorithms revealed that the GWO attained the lowest mean square error (MSE = 0.0028) and exhibited the quickest convergence, establishing it as the most effective algorithm for predicting chloride migration resistance.

c MVO and PSO demonstrated competitive performance, while BAT and CS exhibited slower

convergence and marginally higher prediction errors, indicating diminished suitability for this application.

d The findings demonstrate that the integrated experimental-computational framework significantly minimizes the requirement for extensive experimental trials and aids in optimizing nano-admixture dosage to achieve maximum durability.

Expanding this research to hybrid nanomaterial systems and integrating multi-objective optimization, such as addressing both strength and chloride diffusion resistance concurrently, may result in a more comprehensive mix design strategy.

**Acknowledgement**

The author is thankful to the Department of Civil Engineering at Oriental college of Technology, Bhopal, India, for all the support.

**Funding**

This research did not receive any specific grant from funding agencies in the public, commercial, or not-for-profit sectors.

**Data availability**

The data that support the findings of this study are available from the corresponding author upon reasonable request.

**References**

1 Kaptan K, Cunha S &Aguiar J, *Sustainability*, 16 (2) (2024) 585.
2 Zou D, Hu Q, Bai Z, Zhang M, Liu T, Zhou A & Li Y, *J Build Eng*, (2026) 115269.
3 Liu H, Yang L, Li Z, Fang D, Sun G, Li Y & Gao D, *Constr Build Mater*, 489 (2025) 142207.
4 Manu K C, Madhushree C, Chandini M S, Shree N, Hemanth S & Jeevan T P, *J Mines Met Fuels*, 73(1) (2025) 189.
5 Hu S, Li S, Wen J, Yuan X & Li F, *Coatings*, 16 (1) (2026) 81.
6 Alexander M &Beushausen H, *Cem Concr Res*, 122 (2019) 17.
7 Qu F, Li W, Dong W, Tam V W & Yu T, *J Build Eng*, 35 (2021) 102074.
8 Pandey J L & Banerjee M, *Anti-Corros Methods Mater*, 45 (1998) 16.
9 Papadakis V G, Fardis M N & Vayenas C G, *ChemEngSci*, 51 (1996) 505.
10 Moreno M, Morris W, Alvarez M &Duffó G, *Corros Sci*, 46 (2004) 2681.
11 Cruz RV, Nishikata A &Tsuru T, *Corros Sci*, 40 (1998) 125.
12 Ann K Y & Song H W, *Corros Sci*, 49 (2007) 4113.
13 Arya C, Buenfeld N & Newman J, *Cem Concr Res*, 20 (1990) 291.
14 Hope BB, Page JA & Poland JS, *Cem Concr Res*, 15 (1985) 863.
15 Ahmad S, *Cem Concr Compos*, 25 (2003) 459.
16 Yuan Q, Shi C, De Schutter G, Audenaert K & Deng D, *Constr Build Mater*, 23 (2009) 1.
17 Shi X, Xie N, Fortune K & Gong J, *Constr Build Mater*, 30 (2012) 125.
18 Kechroud F, Benzaamia A & Ghrici M, *Asian J Civ Eng*, (2025) 1.
19 Mapa DG, Zhu H, Nosouhian F, Shanahan N, Riding KA & Zayed A, *Constr Build Mater*, 388 (2023) 131584.
20 Huang Y, Ji F, Chen ZL, Li W & Yu J, *J Build Eng*, 91 (2024) 109587.
21 Rawat G, Gandhi S & Murthy YI, *ACI Mater J*, 120 (2023) 25.
22 Rawat G, Gandhi S & Murthy YI, *Asian J Civ Eng*, 23 (2022) 1197.
23 Rawat G, Gandhi S & Murthy YI, *Emerg Mater Res*, 11 (2022) 495.
24 Rawat G, Gandhi S & Murthy YI, *Građevinar*, 74 (2022) 553.
25 Kim J, *Appl Soft Comput*, 175 (2025) 113110.
26 Murthy YI, *J Soft Comput Civ Eng*, 8 (1) (2024) 85.
27 Yang X & Wang Y, *Multiscale Multidiscip Model Exp Des*, 7(6) (2024) 6289.
28 Sun S, *J Eng Appl Sci*, 72(1) (2025) 93.
29 Li Y, Yang X, Ren C, Wang L & Ning X, *Buildings*, 14(5) (2024) 1209.
30 Kumar N, Prakash S, Ghani S, Gupta M & Saharan S, *Asian J CivEng*, 25 (4) (2024) 3263.
31 Wang F & Zhao J, *Adv Concr Constr*, 19(2) (2025) 75.
32 Sun B, Li Y & Guo T, *Appl Soft Comput*, 157 (2024) 111552.
33 Urkude N, Hora MS &Utkarsh, *Mech Adv Mater Struct*, 32 (15) (2025) 3591.
34 Çiftçioğlu AÖ, Kazemi F &Shafighfard T, *Appl Mater Today*, 42 (2025) 102601.
35 Oh BH & Jang SY, *Cem Concr Res*, 37 (2007) 47.
36 Li L-Y, Xia J & Lin S-S, *Constr Build Mater*, 26 (2012) 295.
37 Wu J, Li H, Wang Z & Liu J, *Constr Build Mater*, 112 (2016) 733.
38 Yu S &Jin H, *Constr Build Mater*, 258 (2020) 119645.
39 Nordtest, *NT Build 492: Concrete, Mortar and Cement-Based Repair Materials – Chloride Migration Coefficient from Non-Steady-State Migration Experiments* (Nordtest, Espoo, Finland), (1999).
40 ASTM, *ASTM C1202-12: Standard Test Method for Electrical Indication of Concrete's Ability to Resist Chloride Ion Penetration* (ASTM International, West Conshohocken, PA), (2012).
41 AASHTO, *T 277-86: Rapid Determination of the Chloride Permeability of Concrete* (American Association of State Highway and Transportation Officials, Washington, DC), (1990).
42 Whiting D, *Rapid Determination of the Chloride Permeability of Concrete* (United States Department of Transportation, Federal Highway Administration), (1981).
43 Andrade C, *Cem Concr Res*, 23 (1993) 724.
44 Yang XS, *Int J Bio-Inspired Comput*, 3 (2011) 267.
45 Gandomi AH, Yang XS & Alavi AH, *Eng Comput*, 29 (1) (2013) 17.
46 Qin AK, Huang VL & Suganthan PN, *IEEE Trans Evol Comput*, 13 (2) (2008) 398.
47 Deng W, Shang S, Cai X, Zhao H, Song Y & Xu J, *Soft Comput*, 25 (7) (2021) 137.

48 Wei X, *Int J Pattern Recognit ArtifIntell*, 40 (10) (2026) 2657010.
49 Alabool HM, Alarabiat D, Abualigah L &Heidari AA, *Neural Comput Appl*, 33(15) (2021) 8939.
50 Houssein EH, Gad AG &Wazery YM, *Metaheuristics and Optimization in Computer and Electrical Engineering*, 3 (2020) 140.
51 Mirjalili S, *Knowl-Based Syst*, 89 (2015) 228.
52 Mirjalili SM & Hatamlou A, *Neural Comput Appl*, 27 (2) (2016) 495.
53 Wang D, Tan D & Liu L, *Soft Comput*, 22 (2) (2018) 387.
54 Mirjalili S, *Knowl-Based Syst*, 96 (2016) 120.
55 Mirjalili SM & Lewis A, *Adv Eng Softw*, 69 (2014) 46.